Maghrebian Journal of Pure and Applied Science
ISSN : 2458-715X
http://revues.imist.ma/?journal=mjpas&page=index

Green approach to corrosion inhibition of mild steel in 1 M HCl solution by Monosaccharides derivatives

A. Methal[1, 2], A. Koulou[1], M. El Bakri[1], M. Ebn Touhami[1], M. Galai, M. Lakhrissi[2], R. Touir[1,*], S. Bakkali

1. Laboratory of Materials Engineering and Environment: Modeling and Application, Faculty of Sciences, University Ibn Tofail, PO Box. 133 – 14000, Kénitra, Morocco

2. Faculty of Science, Laboratory of Agroressources and genius of the processes, PO Box 133, Kénitra, Morocco

* Corresponding author: Tel.: + 212 670 52 69 59.

E-mail address: touir8@yahoo.fr & touir8@gmail.com

Received 14 Oct 2015, Revised 15 Nov 2015, Accepted 16 Nov 2015

Abstract

Effect of new synthesized monosaccharide derivatives, namely: D-mannose (M1), D-gluconic acid-γ-lactone (M2), D-galactono-γ-lactone (M3), monoacetoneglucose (M4), diacetoneglucose (M5), on mild steel corrosion inhibition in an aerated acidic solution of 1 M HCl was investigated using weight loss, potentiodynamic polarization curves, and electrochemical impedance spectroscopy measurements. The results indicate that the type of inhibition depends on the type of compounds. Impedance measurements showed that the charge transfer resistance increased and double layer capacitance values decreased with inhibitor's concentration. It is seen that the M2 performed excellently as a corrosion inhibitor which its efficiency reaches 91 % at 10^{-3} M. Adsorption of M2 molecules on mild steel surface was also studied to examine basic information on the interaction between the inhibitors and the metal surface. It is found that the inhibitor adsorb on the metal surface following the Langmuir isotherm model. The temperature effect on the performance of mild steel in 1 M HCl in the absence and presence of the best compound was studied in the temperature range from 293 to 323 K. Also, some thermodynamic data for the adsorption and dissolution processes are calculated and discussed.

Keywords: Corrosion inhibition, EIS, Monosaccharide derivatives, mild Steel, Hydrochloride acid

1. Introduction

The search and application for new and efficient corrosion inhibitors is necessary to secure metallic materials against corrosion. The selection of appropriate inhibitors mainly depends on the formulation as well as rational use in various environments. The degree of metal protection is a function of metal adsorption [1]. The adsorption behavior of inhibitor molecules on metallic surfaces will be affected by their molecular structure, surface state and surface excess metal charge, chemical composition of solution, temperature of the reaction, immersion time and electrochemical potential at the metal/solution interface [2].

Recently, many workers have reoriented their attention to the development of new corrosion inhibitors based on organic compounds having multiple bonds in their molecules, which mainly contain nitrogen and sulfur atoms through which they are adsorbed on the metal surface. Among these, several triazoles [3-5], tetrazole [6, 7],

pyrazoles [8], imidazoles [9–11], pyridazines [12, 13], quinoxaline [14-17], Isoindoline [7], benzamide derivatives [18] etc. have been among the best known and the most studied inhibitors.

The choice of these compounds was based on the consideration that theses compounds are generally heterocyclic compounds containing nitrogen, sulfur and/or oxygen atoms, triple bounds or aromatic rings which induce greater adsorption of the inhibitor molecules onto the surface of carbon and meld steel, leading to the formation of a corrosion protecting film [19].

However, majority of these organic compounds are toxic for human being and environment as well. The new generation of environmental regulation requires the replacement of toxic inhibitor with non toxic inhibitor. That's why the naturally occurring substances of both plant and animal origin have been found to satisfy this need. M.S. Al-Otaibia and al. [20] has given comprehensive review of natural products as corrosion inhibitors for metals in acidic media. From a historical point of view, natural products (e.g., polysaccharides) have been the first corrosion inhibitors at all [21]. Saccharides (sugars) are renewable raw materials and absolutely non-toxic. Glucose (grape sugar) has been used as corrosion inhibitor for aluminum metal in alkaline medium [21]. Ascorbic acid (vitamin C) is technically synthesized from glucose and can be considered as a saccharide derivative [22] as well as salts of isoascorbic acid [23] has been described as corrosion inhibitors for iron.

Moreover, there is generally a great demand for environmentally friendly corrosion inhibitors (so called "green inhibitor"), for example, Carboxymethyl cellulose (CMC) has been reported to inhibit the corrosion of Cadmium [24] and mild steel in HCl solution [25]. In addition, gluconates and gluconic acid are known to be effective non-toxic inhibitors for iron and mild steel in cooling water systems [26-28]. It is found that inhibition efficiencies of the monosaccharides derivatives do not only depend on its structure, but also on the characteristics of the environment in which it acts the nature of metal and other experimental conditions [28].

In response to environmental guidelines, the purpose of this work is to investigate the ability of new inhibitors (monosaccharide derivatives) as corrosion inhibitor for mild steel in 1 M HCl solution using electrochemical techniques and weight loss measurements. The effect of temperature was investigated. In addition, adsorption of the best inhibitor on mild steel surface was also studied to examine basic information about the interaction between the inhibitor and the metal surface.

2. Experimental details

2.1 Material preparation

Corrosion tests were performed on a mild steel which had the following chemical composition (wt. %): C=0.21, Si=0.38, P=0.09, Mn=0.05, S=0.05, Al=0.01, and the remainder iron. The specimen's surface was prepared by grinding with emery paper at different grit sizes (from 180 to 1200), rinsing with distilled water, degreasing in ethanol, and drying before use. The aggressive solution of 1 M HCl was prepared by dilution of analytical grade 37 % HCl with distilled water. The molecular formula of the examined inhibitor is shown in Table 1. Their concentrations range was from 10^{-5} M to 10^{-2} M.

Table 1. The chemical formulas of the investigated molecular.

Serial	Monosaccharide	Structural formula	Abréviation	Molar mass
1st serial	D-mannose	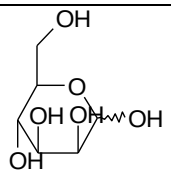	M1	180
2nd serial	D-gluconic acid-γ-lactone	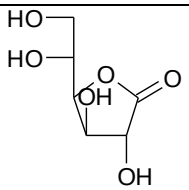	M2	178

	D-galactono-γ-lactone	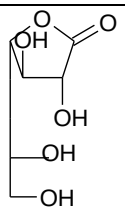	M3	178
3rd serial	monoacetoneglucose	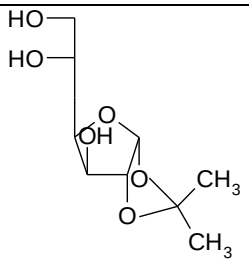	M4	220
	diacetoneglucose	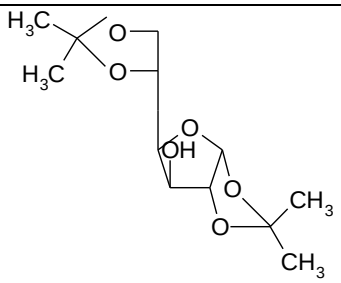	M5	260

2.2. Measurements

2.2.1. Weight loss measurements

Weight loss measurements were carried out in an electrolysis cell closed by a cap with five apertures and equipped with a thermostat-cooling condenser. The mild steel specimens used have a rectangular form (length = 2.9 cm, width = 1 cm, thickness = 0.05cm). The immersion time for weight loss was 24 h at 298 K. After immersion period, the specimens were cleaned according to ASTM G-81 and reweighed to 10^{-4} g for determining corrosion rate [29]. The inhibition efficiency, ηw%, is defined as follows, Eq. (1):

$$\eta_W\,\% = \frac{w^0_{corr} - w_{corr}}{w^0_{corr}} \times 100 \qquad (1)$$

where w^0_{corr} and w_{corr} are the corrosion rates without and with inhibitor, respectively.

2.2.2. Electrochemical measurements

For electrochemical measurements, the electrolysis cell was a borrosilcate glass (Pyrex®) cylinder closed by a cap with five apertures. Three of them were used for the electrode insertions. The working electrode was pressure-fitted into a polytetrafluoroethylene holder (PTFE) exposing only 1 cm^2 of surface to the solution. Platinum and saturated calomel were used as counter and reference electrode (SCE), respectively. All potentials were measured against this later electrode.

The potentiodynamic polarization curves were recorded by changing the electrode potential automatically from negative to positive values versus E_{corr} using a Potentiostat/Galvanostat type PGZ 100, at a scan rate of 1 mV/s after 1 h of immersion time until reaching steady state. The test solution was thermostatically controlled at 298 K in air atmosphere without bubbling.

From the polarization curves obtained, the corrosion current (i_{corr}) was calculated by curve fitting using the Stern–Geary, Eq. (2):

$$i = i_a + i_c = i_{corr} \times \left\{ \exp\left[b_a \times \left(E - E_{corr}\right)\right] - \exp\left[b_c \times \left(E - E_{corr}\right)\right] \right\} \qquad (2)$$

where i_{corr} is the corrosion current density (A cm^{-2}), and b_a and b_c are the Tafel constants of the anodic and cathodic reactions (V^{-1}), respectively. These constants are related to the Tafel slope β (V dec^{-1}) in the usual logarithmic scale by Eq. (3)

$$b = \frac{\ln(10)}{\beta} \approx \frac{2.303}{\beta} \qquad (3)$$

The inhibition efficiency was then evaluated from i_{corr} values determined using the following relationship, Eq. (4):

$$\eta_{EIS}\,\% = \frac{i_{corr}^{0} - i_{corr}}{i_{corr}^{0}} \times 100 \qquad (4)$$

The surface coverage values (θ) have been obtained from polarization curves for various concentrations of inhibitor using the following equation [30]:

$$\theta = 1 - \frac{i_{corr}}{i_{corr}^{0}} \qquad (5)$$

where the superscript 0 indicates the corrosion current densities relative to that determined in the absence of inhibitor.

The electrochemical impedance spectroscopy measurements were made at the open-circuit potential (OCP) were carried out using a transfer function analyzer (VoltaLab PGZ 100; Radiometer Analytical), with a small amplitude ac signal (10 mV rms), over a frequency domain from 100 kHz to 10 mHz with ten points per decade at 293 K. The impedance diagrams were given in the Nyquist representation. The results were then analyzed in terms of equivalent electrical circuit using Bouckamp's program [31]. The inhibition efficiency was evaluated using the relationship:

$$\eta\% = \frac{R_{tc} - R_{tc}^{0}}{R_{tc}} \times 100 \qquad (6)$$

where R^{0}_{tc} and R_{tc} are the charge transfer resistance values without and with inhibitor, respectively.

In order to ensure reproducibility, all experiments were repeated three times. The evaluated inaccuracy did not exceed 10 %.

3. Results and discussions

3.1. Weight loss measurements

The effect of monosaccharide derivatives on mild steel corrosion in 1 M HCl was studied by weight loss at 293 K. The obtained results are presented in Table 2. It is seen that the inhibition efficiency increases with concentration and reaches a maximum 37 %, 62 %, 74 %, 74 % and 90 % at 10^{-2} M of M4, M1, M3, M5 and M2, respectively. This behavior could be attributed due to strong interaction via adsorption between compound and metallic surface [32]. This may also be due to the inhibitor adsorption at the mild steel surface through non-bonding electron pairs present on nitrogen, oxygen, and sulfur atoms as well as π-electrons [33]. Other authors showed that molecular area [34] and molecular weight [35] of the organic molecule have an effect on the corrosion inhibition of metals in acidic solutions.

However, the variation of inhibition efficiency mainly depends on the number and position of group -OH in the monosaccharide i.e. with molecular size such as mentioned in our previously study [28]. However, the high inhibitive performance of M2 suggests a higher bonding ability on the mild steel surface, which possesses higher numbers of lone pairs of oxygen atom present in the monosaccharide. The electron lone pair on the oxygen will co-ordinate with the metal atoms of the active sites, causing a stronger interaction with the metal

surface, and it was found that η_w (%) increases with electron density. The oxygen atom can donate π-electrons to the metal surface and increase adsorption and hence higher inhibition efficiency. So, from weight loss measurements, we can conclude that the inhibition efficiency of the five tested monosaccharide flow the order: M2 > M5 ≈ M3 > M1 > M4.

Table 2. Gravimetric results for mild steel in 1 M HCl without and with different concentrations of different monosaccharide compounds.

Inhibitors	Conc. (M)	W_{corr} (mg cm^{-2} h^{-1})	η_w(%)
Blank solution	00	0.0048	-
D-mannose (M1)	10^{-4}	0.0034	28
	10^{-3}	0.0023	52
	10^{-2}	0.0018	62
D-gluconic acid-γ-lactone (M2)	10^{-4}	0.0006	87
	10^{-3}	0.0005	88
	10^{-2}	0.0004	90
D-galactono-γ-lactone (M3)	10^{-4}	0.0062	-
	10^{-3}	0.0017	64
	10^{-2}	0.0025	74
Monoacetoneglucose (M4)	10^{-4}	0.0017	64
	10^{-3}	0.0012	75
	10^{-2}	0.0030	37
Diacetoneglucose (M5)	10^{-4}	0.0067	64
	10^{-3}	0.0057	70
	10^{-2}	0.0014	74

3.2. Potentiodynamic polarization curves

Potentiodynamic polarisation curves of mild steel in 1 M HCl without and with different concentrations of monosaccharide derivatives at 293K are shown in figure 1. Their corresponding data, percentage inhibition efficiency (η_{IE}%) and surface coverage values (θ) are given in the Table 2.

From the recorded results, we can conclude that, in all cases, addition of the studied M1, M2 and M5 induced a marked decrease in corrosion current density (i_{corr}). In addition, it is noted that the anodic current densities of M1 decreases indicating that this inhibitor act on the electrode dissolution reactions such as anodic-type inhibitors while that of M2, M3, M4 and M5 compounds act as cathodic inhibitors. It is also seen from these results that these inhibitors decrease i_{corr} values in the concentration range of 10^{-5}- 10^{-4} M concentration. Maximum reduction of i_{corr} for these inhibitors is obtained at 10^{-2} M of M2. However, the inhibitor additions does not change the cathodic hydrogen evolution reaction mechanism such as indicated by the slight changes in (βc) values. This indicates that hydrogen evolution is activation controlled [36, 37].

It is evident from the data that inhibition efficiency (η_{IE}%) increases with concentration inhibitors and reaches of 87% at 10^{-2} M of M2 due to the increase in the blocked fraction of the electrode surface by adsorption [38]. This increase indicate that the presence of excess oxygen atoms and the presence of aromatic ring in M2 compared to the other compounds, which can increases the adsorption of molecules on mild steel surface and give more inhibitions such as mentioned above. The same order was observed in this case which is : M2 > M5 ≈ M3 > M1 > M4. In addition, this order can be explained by the number of free –OH group and hydrogen liaison such as mentioned in our previous study [28].

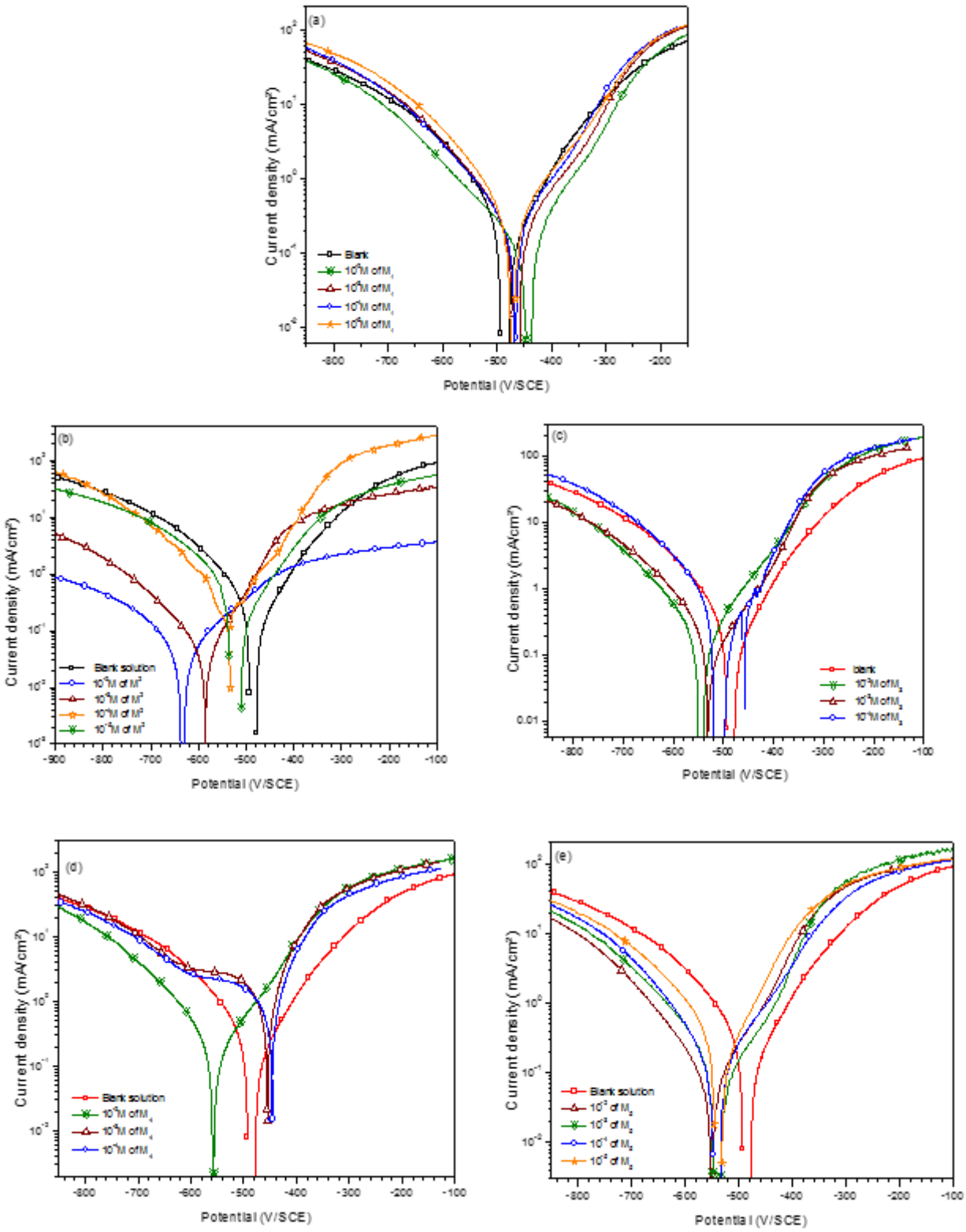

Figure 1: Potentiodynamic polarization curves for mild steel in 1M HCl containing different concentration of (a) M1, (b) M2, (c) M3, M4 and (e) M4.

3. 3. Electrochemical Impedance Spectroscopy (EIS)

Impedance measurements provide information on both the resistive and capacitive behavior of the interface and makes possible to evaluate the performance of the studied inhibitors. The electrochemical process occurring at the open-circuit potential (OCP) was examined by electrochemical Impedance spectroscopy (EIS). The

influence of the different investigated organic compounds on mild steel corrosion in 1 M HCl by EIS is shown in Fig. 2.

Table 3. Electrochemical parameters for mild steel in 1 M HCl at various concentrations of monosaccharide substituted compounds at 293 K

Inhibitors	Conc. (M)	Ecorr (mV/SCE)	i_{corr} ($\mu A/cm^2$)	βa (mV dec^{-1})	-βc (mV dec^{-1})	η_{IE} (%)	Θ (%)
Blank	-	-486	0.574	97	143	-	-
D mannose (M1)	10^{-5}	-472	0.512	102	123	11	0.1080
	10^{-4}	-466	0.290	85	127	49	0.4947
	10^{-3}	-464	0.282	90	131	51	0.5087
	10^{-2}	-443	0.105	85	143	82	0.8170
D-gluconic acid-γ-lactone (M2)	10^{-5}	-519	0.483	84	136	16	0.1585
	10^{-4}	-534	0.442	82	176	23	0.2299
	10^{-3}	-586	0.074	131	184	87	0.8710
	10^{-2}	-634	0.072	73	175	87	0.8745
D-galactono-γ-lactone (M3)	10^{-4}	-510	0.928	62	96	-	-
	10^{-3}	-530	0.443	84	148	23	0.2282
	10^{-2}	-544	0.355	74	162	38	0.3815
Monoacetoneglucose (M4)	10^{-4}	-455	1.894	46	223	-	-
	10^{-3}	-446	1.486	48	233	-	-
	10^{-2}	-557	0.415	85	131	28	0.2770
Diacetoneglucose (M5)	10-5	-538	0.312	63	139	46	0.4564
	10-4	-540	0.199	54	144	65	0.6533
	10-3	-541	0.196	85	123	66	0.6566
	10-2	-541	0.098	68	143	83	0.8222

The same trend (one capacitive loop) was also observed for mild steel immersed in 1 M HCl without and with monosaccharide compounds at different concentration, indicating that almost no change in the corrosion mechanism occurred with inhibitors addition. This behavior can be attributed to charge transfer of the corrosion process. It is also noticeable that the diameter of the semicircle increases with inhibitor concentration, indicating an increase in corrosion resistance of the material [39]. The transfer function can be represented by a resistance R_1 parallel to a capacitor C and in series to them an additional resistance R_2 as expressed in equation (7):

$$Z(W) = R_1 + (\frac{1}{R_2} + jWC)^{-1} \qquad (7)$$

This transfer function is applicable for homogeneous systems with one time constant when the center of the semicircle lies on the abscissa of real part. It is evident that it cannot describe the observed depression of the capacitive loop and it is necessary to replace the capacitor by some element taking into account frequency dispersion like the Constant Phase Element (CPE). This element is a generalised tool, which can reflect exponential distribution of the parameters of the electrochemical reaction related to energetic barrier at charge and mass transfer. Such phenomena often correspond to frequency dispersion [40] imputed to different physical phenomena, such as roughness and non-homogeneities of the solid surface. In order to fit and analyze the EIS data, the equivalent circuit shown in Fig. 3 is selected.

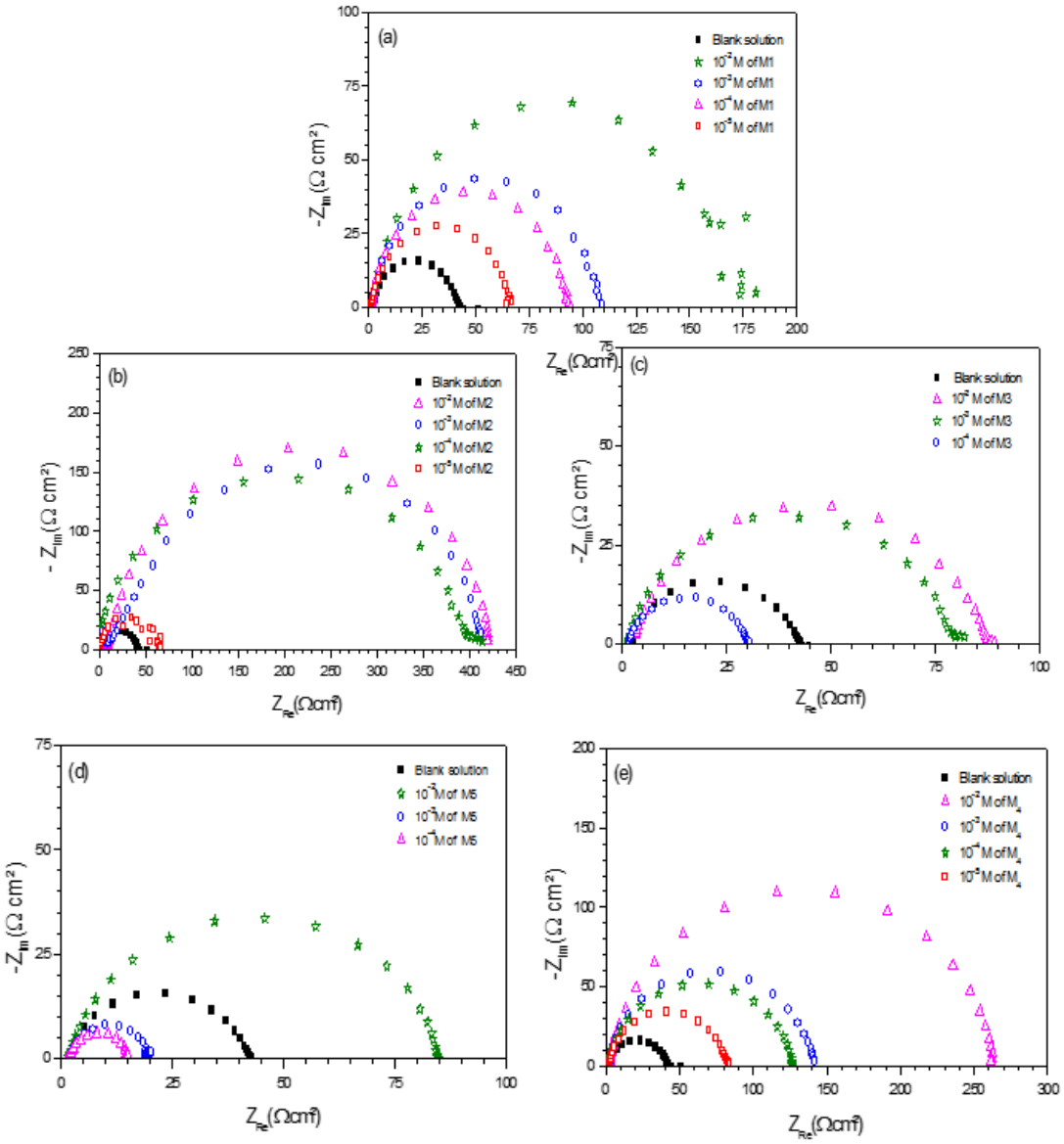

Figure 2: Nyquist plots for mild steel in 1 M HCl solution at 293K in absence and presence of various concentrations of (a) M1, (b) M2 , (c) M3, (d) M4 and (e) M5.

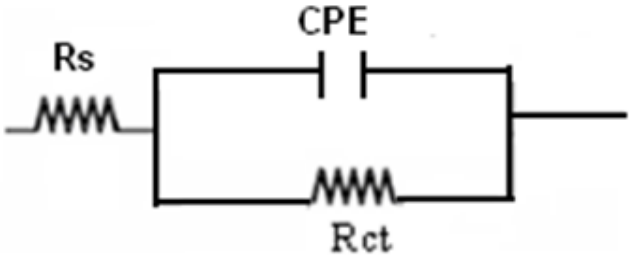

Figure 3: Equivalent circuit model for system mild steel/1 M HCl/inhibitor.

This circuit is generally used to describe the iron/acid interface model [41]. In this equivalent circuit, R_{ct} reflects the charge transfer resistance R_2, R_s is the resistance of the solution R_1, and (CPE) is a constant phase element related to the capacity of the double layer. The CPE is defined by the mathematical expression [42, 43]:

$$Z_{CPE} = A^{-1}(iw)^{-n} \qquad (8)$$

where A is the CPE constant, w is the angular frequency (rad s^{-1}), $i^2 = -1$ is the imaginary number, and n is a CPE exponent which can be used as a gauge of the heterogeneity or roughness of the surface [44]. Depending on the n value, CPE can represent resistance (n = 0, A = R), capacitance (n = 1, A = C), inductance (n = -1, A = L), or Warburg impedance (n = 0.5, A = W). In addition, the double layer capacitance values, C_{dl}, calculated from CPE data by use of Eq. (9) [45] are listed in Table 4.

$$C_{dl} = (AR_{ct}^{\,1-n})^{1/n} \qquad (9)$$

Table 4 shows that inhibitor addition increases the R_{ct} values (the greatest effect 437 Ω cm^2 was observed at 10^{-2} M of D-gluconic acid- γ-lactone (M2)) indicated that charge transfer process mainly controls the corrosion process. The decrease in C_{dl} values indicated that the inhibitor function by adsorption at the metal/solution interface originally by gradual displacement of water molecules and/or chloride ions on the mild steel surface [44], leading to a protective solid film, inhibiting species or both on the mild steel surface, then decreasing the extent of dissolution reaction [41,45]. This decrease of C_{dl} concentration can be explained by the decrease in local dielectric constant and/or an increase in the protective layer thickness on the electrode surface. This trend is in accordance with Helmhotz model, given by the following equation [46].

$$C_{dl} = \frac{\varepsilon_0 \varepsilon}{e} S \qquad (10)$$

ε is the dielectric constant of the protective layer, ε_0 is the permittivity of free space (8.854×10^{-14} F cm^{-1}) and S is the effective surface area of the electrode

In addition, the inhibition efficiencies increase with concentration and the D-gluconic acid- γ-lactone (M2) is the best.

Table 4. Characteristic parameters evaluated from impedance diagram for mild steel in 1 M HCl with and without various concentrations of monosaccharide substituted compounds at 298 K.

Inhibitors	Conc. (M)	R_{tc} (Ω cm^2)	C_{dl} (μF/cm^2)	η_{EIS} (%)	Θ (%)
Blank solution	-	41	345	-	
D mannose (M1)	10^{-5}	67	143	39	0.3880
	10^{-4}	94	102	56	0.5638
	10^{-3}	109	87	62	0.6238
	10^{-2}	171	79	76	0.7602
D-gluconic acid-γ-lactone (M2)	10^{-5}	66	291	38	0.3787
	10^{-4}	394	48	89	0.8960
	10^{-3}	425	45	90	0.9029
	10^{-2}	437	40	91	0.9054
D-galactono-γ-lactone (M3)	10^{-4}	29	146	-41	-0.4137
	10^{-3}	80	81	49	0.4875
	10^{-2}	88	74	53	0.5326
Monoacetoneglucose (M4)	10^{-4}	15	371	-173	-1.7333
	10^{-3}	18	360	-56	-0.5609
	10^{-2}	85	240	52	0.5176
Diacetoneglucose (M5)	10^{-5}	85	116	52	0.5176
	10^{-4}	128	148	68	0.6796
	10^{-3}	141	75	71	0.7092
	10^{-2}	266	53	85	0.8458

Generally, two modes of adsorption can be considered. The process of physical adsorption requires the presence of electrically charged metal surface and the charged species in the bulk of the solution. Chemisorption process involves charge sharing of charge transfer from the inhibitor molecules to the metal surface. This is possible in case of positive as well as negative charges on the surface. The presence of a transition metal, having vacant, low-energy electron orbital, and an inhibitor molecule having relatively loosed bound electrons or heteroatoms with lone-pair electrons facilitates this adsorption [47]. For this, M2 which possess oxygen atoms and lone-pair electrons, can accept a proton, leading the cationic forms. These species can adsorb on the metal surface because of attractive forces between the negatively charged metal and the positively inhibitors.

3.4. Thermodynamic parameters of the adsorption process for M2

The adsorption isotherm type can provide additional information about the tested compounds properties. The fractional coverage surface (θ) can be easily determined from, Tafel polarization or the linear polarization. In the present study, the θ evaluated from impedance measurements (Table 4). The adsorption isotherms models considered were as described in reference [48]:

Temkin isotherm
$$\exp(f\theta) = K_{ads}C_{inh} \quad (11)$$

Langmuir isotherm
$$\frac{\theta}{1-\theta} = K_{ads}C_{inh} \quad (12)$$

Frumkin isotherm
$$\frac{\theta}{1-\theta}\exp(-2f\theta) = K_{ads}C_{inh} \quad (13)$$

Freundluich isotherm
$$\theta = K_{ads}C_{inh} \quad (14)$$

where K_{ads} is the equilibrium constant of the adsorption process, C_{inh} is the inhibitor concentration and f is the factor of energetic inhomogeneity. The linear coefficient regression (LCR), r^2 and the slope, were used to choose the suitable isotherm (Table 5). K_{ads}, is related to the free energy of adsorption, ΔG^*_{ads}, by the following equation (15) [49]:

$$K_{ads} = \frac{1}{55{,}55}\exp\left(-\frac{\Delta G^*_{ads}}{RT}\right) \quad (15)$$

where 55.55 represents the water concentration in solution in mol L^{-1}, R is the universal gas constant and T is the absolute temperature.

The best fit straight line (strong correlation with $r \approx 1$) is obtained for the plot of C_{inh}/θ vs. C_{inh} with slopes around unity (Figure 4). This suggests that the adsorption of M2 (best inhibitor) on metallic surface obeyed to the Langmuir's adsorption isotherm model, and exhibit single-layer adsorption characteristics. This kind of isotherm involves the assumption of no interaction between the adsorbed species on the electrode surface [49]. The values of K_{ads}, LCR, and ΔG^*_{ads}, are calculated and are given in Table 5. The high K_{ads} values reflect the high adsorption ability of this inhibitor on metallic surface. In addition, the negative values of free energy of adsorption, ΔG^*_{ads}, indicate spontaneous adsorption of M2 molecules on the metallic surface and also the strong interaction between inhibitor molecules and the mild steel surface [50, 51]. Generally, the standard free energy values of -20 KJ mol^{-1}or less negative are associated with an electrostatic interaction between charged molecules and charged metal surface (physical adsorption); those of -40 KJ mol^{-1}or more negative involve charge sharing or transfer from the inhibitor molecules to the metal surface to form a co-ordinate covalent bond (chemical adsorption) [52, 53]. Based on the literature [54], the calculated ΔG^*_{ads} values in this work indicate that the adsorption mechanism of M2 on mild steel surface in 1 M HCl solution involves two types of interaction, electrostatic-adsorption (ionic) and chemisorption (molecular) [55].

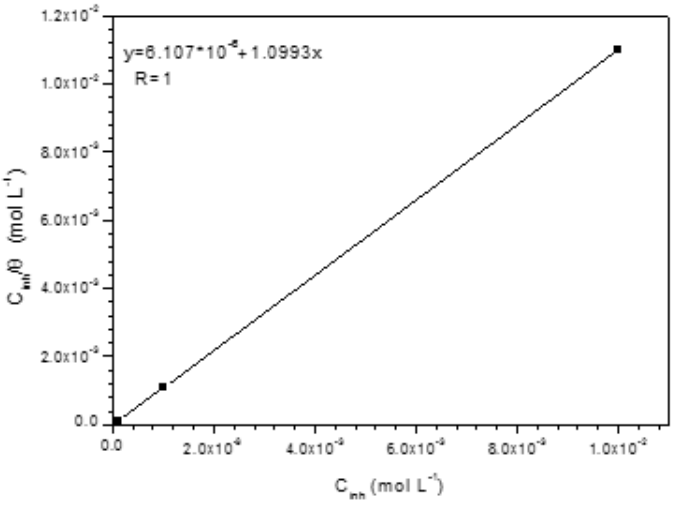

Figure 4. Langmuir adsorption isotherm plot for mild steel in 1 M HCl at different concentrations of M2

Table 5. Equilibrium constant and free energy of adsorption values for mild steel in 1 M HCl in presence of M2

Inhibitor	Slope	K_{ads} (L mol^{-1})	ΔG^*_{ads} (KJ.mol^{-1})	L.C.R (r)
M2	1.09	16.37×104	-39.69	1

3.5. Thermodynamic parameters of the activation corrosion process for M2

In order to gain more information about the adsorption type of M2 and its effectiveness at higher temperatures, potentiodynamic polarization measurements were used in the temperatures range from 293 to 323 K for mild steel electrode in 1 M HCl without and with 10^{-2} M of M2 after an hour of time immersion. The obtained results are presented in Fig. 5. Their corresponding data are collected in Table 6. It is noticed that the increase of solution temperature leads to increase in current density values of the two branches of the polarization curves and consequently the values of i_{corr}. However, the increase in current density is highly more pronounced in uninhibited than in inhibited media. Indeed, it is worth noting that the values of i_{corr} in the presence 10^{-2} M of M2 are always weaker than in its absence. Moreover, no clear trends are observed in E_{corr} values at higher temperatures in free medium and with M2 inhibitor. These results reflect the enhancement of both the cathodic hydrogen evolution reaction as well as anodic mild steel dissolution with the rise of temperature.

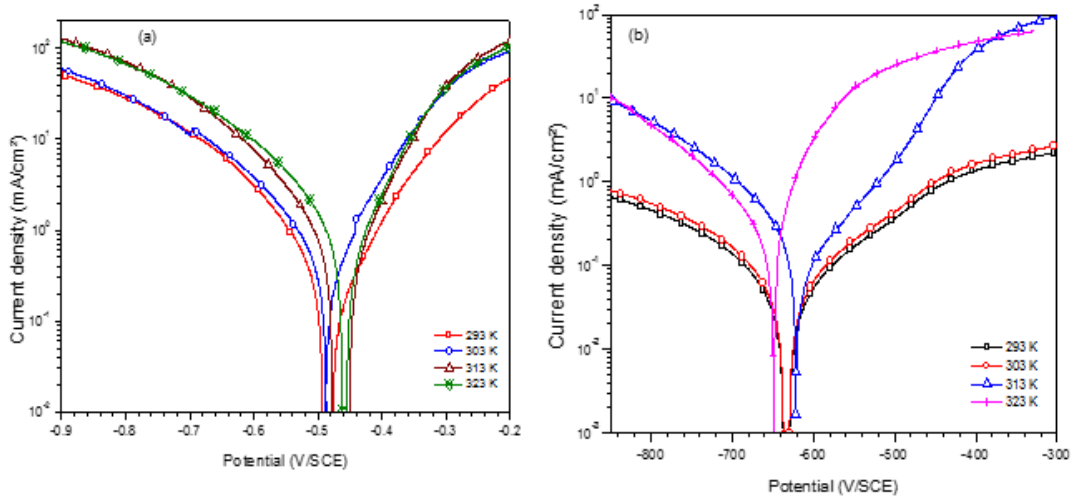

Figure 5. Effect of temperature on the behaviour of mild steel / 1M HCl interface in (a) uninhibited solution, (b) in the presence of 10^{-4} M of M2

Table 6. Electrochemical characteristics of mild steel in 1 M HCl with and without 10^{-4} M of M2 at different temperatures

Temperature (K)	Conc. (M)	E_{corr} (mV/SCE)	i_{corr} (mA/cm2)	η_p (%)	θ
293	0	-486	0.574	-	-
	10^{-2}	-634	0.072	87	0.8745
303	0	-490	0.808	-	-
	10^{-2}	-634	0.096	88	0.8811
313	0	-465	1.177	-	-
	10^{-2}	-648	0.416	65	0.6465
323	0	-456	1.591	-	-
	10^{-2}	-622	0.424	73	0.7335

However, data in table 6 revealed that M2 exhibited inhibition efficiency at all the studied temperature and the values of inhibition efficiency; η_{IE}(%) slightly increase with temperature in the range from 293 to 303 and decrease in the range from 303 to 323. These behaviors, together with the higher adsorption equilibrium constant Kads values (Table 5) confirm the chemisorption M2 on the mild steel surface. This result has been explained by some authors as likely specific interaction between the iron surface and the inhibitor. Ivanov [56] explains this increase with temperature by the change in the nature of the adsorption mode; the inhibitor is being physically adsorbed at lower temperatures, while chemisorption is favored by increasing of temperature. The same phenomenon was explained by other workers as an increase in the surface coverage by the inhibitor [57]. Thus, at a high surface coverage values, the diffusion through the surface layer containing the inhibitor and corrosion products becomes the rate-determining step of the metal dissolution process [58]. Thus, the inhibition properties of M2 can be explained by kinetic model. The dependence of the corrosion value i_{corr} on the temperature can be regarded as Arrhenius-type process given by equation (16) [59]:

$$\ln i_{corr} = \ln A - \frac{E_a}{RT} \qquad (16)$$

where E_a is the apparent activation energy of corrosion process, R is the universal gas constant, A is the Arrhenius pre-exponential constant and T is the absolute temperature.

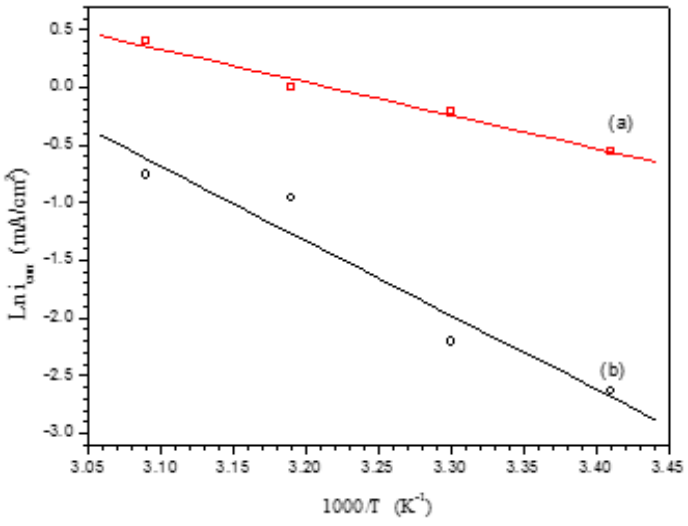

Figure 6: Arrhenius plots of mild steel in 1 M HCl (a) without and (b) with 10^{-2} M of M2

In order to assure that the achieved coverage degree is close to the maximal value; i.e. the concentration which gives the best inhibiting efficiency The Arrhenius plot according to equation (16) is presented in Fig. 6 in the absence and presence of 10^{-2} M of M2. The apparent activation energy values (E_a) for mild steel in 1 M HCl in the absence and presence of 10^{-2} M of M2 were determined from the slope of Ln i_{corr} vs. 1/T plots and shown in Table 7 which include as well the pre-exponential term, A. All the linear regression coefficients between Ln i_{corr} vs. 1/T are very close to one, indicating that the mild steel corrosion in 1 M HCl solution can be elucidated using the kinetic model.

Table 7. The values of activation parameters E_a, ΔH_a^* and ΔSa^* for mild steel in 1M HCl in the absence and presence of 10^{-2} M of M2.

	Pre-exponential factor, A ($\mu A\ cm^{-2}$)	E_a KJ mol^{-1}	ΔH_a^* KJ mol^{-1}	ΔS_a^* J K^{-1} mol^{-1}
Blank sàlution	0.97×10^4	23.47	21.28	-176.82
M2	0.23×10^4	53.51	50.89	-93.53

The values of A as well as E_a in the presence of inhibitor follow the same trend and are higher than those in uninhibited solution. So the decrease in mild steel corrosion rate is determined by the apparent activation energy, E_a value. It is well recognized that the temperature dependence of the inhibition effect and the comparison of the values of the apparent activation energy, E_a, of the corrosion process in absence and presence of inhibitors can provide further evidence [62, 63] concerning the mechanism of the inhibition action. The decrease of the inhibitor efficiency with temperature, which refers to a higher value of E_a, when compared to free solution, is interpreted as an indication for an electrostatic character of the inhibitor's adsorption. From the Table 7, the addition of M2 affects the values of E_a; this modification may be attributed to the change in the corrosion process mechanism in the presence of adsorbed inhibitor molecules [46].

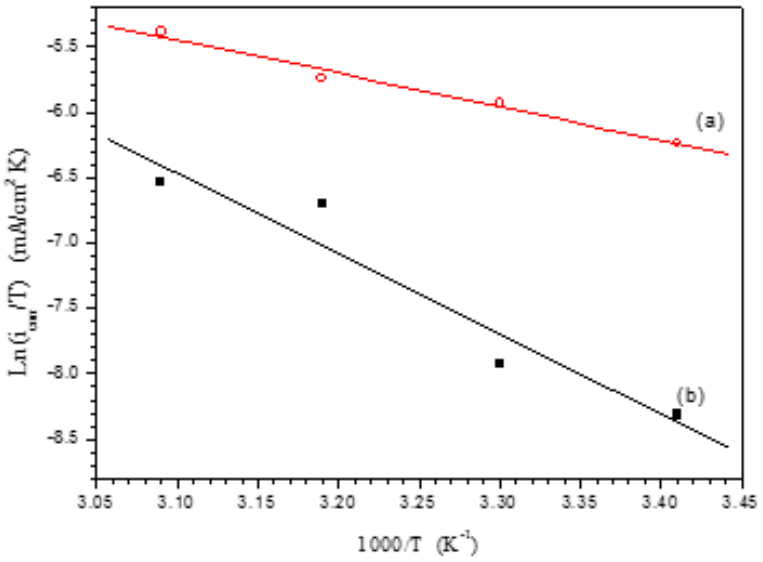

Figure 7. Arrhenius plots of Ln(i_{corr}/T) vs. 1/T for mild steel in 1 M HCl (a) without and (b) with 10^{-2} M of M2

The value of E_a was greater than 20 KJ mol^{-1}, which reveals that the entire process is controlled by the surface reaction [62].The investigated inhibitor block significantly some of the active sites on the metal surface inhomogeneous energetically. In general, the inhibitor adsorbs at the most active sites of the surface with lowest E_a and thus isolates them. Other active sites of higher E_a take part in the further corrosion process.
Other kinetic data are accessible using the alternative formulation of the Arrhenius equation is (17) [63]:

$$\ln\frac{i_{corr}}{T} = \left(\ln\left(\frac{R}{Nh}\right) + \frac{\Delta S_a^*}{R}\right) - \frac{\Delta H_a^*}{RT} \qquad (17)$$

where h is Plank's constant, N is Avogadro's number, ΔS_a^* is the entropy of activation and ΔH_a^* is the enthalpy of activation. Plots of Ln (i_{corr}/T) vs. 1/T are presented in Fig. 7 for mild steel in 1M HCl in the absence and presence of 10^{-2} M of M2. Straight lines are obtained with a slope of ($-\Delta H_a^*/R$) and an intercept of ($LnR/Nh + \Delta S_a^*/R$). The values of ΔH_a^* and ΔS_a^* are calculated and are listed in Table 7. The positive sign of the enthalpies ΔH_a^* reflects the endothermic nature of the steel dissolution process whereas large negative values of entropies ΔS_a^* imply that the activated complex in the rate determining step represents an association rather than a dissociation step, meaning that a decrease in disordering takes place on going from reactants to the activated complex [63-65].

4. Conclusion

From the above results and discussions, the following conclusions can be drawn:

1. Reasonably good agreement was observed between the obtained data from weight loss, potentiodynamic polarization curves and electrochemical impedance spectroscopy techniques.
2. The obtained results show that the all monosaccharide derivatives act as inhibitors for mild steel in 1 M HCl.
3. Polarization measurements showed that the inhibitor M2, M3, M4 and M5 are a cathodic type, but M1 acts as a mixed type inhibitor.
4. EIS measurements also indicate that the inhibitors addition increases the charge transfer resistance and show that the inhibitive performance depends on molecules structure.
5. The values of inhibition efficiency obtained show that the best inhibition is M2 than other compounds and this can be explained by the number of free –OH group and hydrogen liaison.
6. The adsorption of M2 on the metal surface is well described by the Langmuir adsorption isotherm model.
7. The value of the standard Gibbs energy of adsorption is negative and lower in absolute values ΔG^*_{ads} than40 $kJmol^{-1}$. This result confirms that both of chemisorption and physisorption control the adsorption phenomenon.
8. The impact of temperature taken together on the corrosion inhibition process demonstrates the double character nature of the adsorption phenomena. There is no evidence to confidently attribute either a chemisorption or a physisorption mechanism for M2.

References

1. O. K. Abiola. **Corros. Sci, 48 3078–3090 (2006).**
2. J.Z. Ali, X.P. Guo, J.E. Qu, Z.Y. Chen, J.S. Zheng. **Colloids Surf. A: Physicochem. Eng. Aspects**, **281, 147–155 (2006)**
3. M. Abouchane M., El Bakri, R. Touir, A. Rochdi, O. Elkhattabi, M. Ebn Touhami, Forssal I., Mernari B. **Res. Chem. Intermed., DOI 10.1007/s11164-013-1319-5 (2013).**
4. M. El Bakri, R. Touir, M. Ebn Touhami, A. Srhiri, M. Benmessaoud. **Corros. Sci. 50, 1538–1545 (2008)**
5. W. Li, Q. He. C. Pei, B. Hou. **Electrochim. Acta, 52, 6386 (2007)**
6. J. Hmimou, A. Rochdi, R. Touir, M. Ebn Touhami, E.H. Rifi, A. El Hallaoui, A. Anouar, D. Chebabe. **J. Mater. Environ. Sci. 3, 543–550 (2012)**
7. Y. Elkacimi, M. Achnin, Y. Aouine, M. Ebn Touhami, A. Alami, R. Touir, M. Sfaira, D. Chebabe, A. Elachqar, B. Hammouti**, Portugaliae Electrochimica Acta, 30(1), 53-65 (2012)**
8. B. Zerga, A. Attayibat, M. Sfaira, M. Taleb, B. Hammouti, M. Ebn Touhami, S. Radi, Z, Rais. , **J.Appl. Electrochem. 40, 1575 (2010)**
9. M. Scendo, M. Hepel. **Corros. Sci. 49, 3381 (2007).**
10. A. Lamkaddem, R. Touir, E.M. Essassi, M. Ebntouhami. **Sci. Study Res. VIII, 19–28 (2007)**
11. L. Larabi, O. Benali, S.M. Mekelleche, Y. Harek. **Appl. Surf. Sci, 253, 1371 (2006)**
12. K. Benbouya, I. Forsal, M. El Bakri, T. Anik, R. Touir, M. Bennajah, D. Chebabe, A. Rochdi, B. Mernari, M. Ebn Touhami. **Res. Chem. Intermed, DOI 10.1007/s11164-013-1037-z (2013)**

13. B. Zerga, R. Saddik, B. Hammouti, M. Taleb, M. Sfaira, M. Ebn Touhami, S.S. Al-Deyab. N. Benchat. **Int. J. Electrochem. Sci, 7, 631 (2012).**
14. K. Adardour, R. Touir, M. El Bakri, H. Larhzil, M. Ebn Touhami, Y. Ramli, A. Zarrouk, H. El Kafsaoui, E. M. Essassi, **Res. Chem. Intermed., DOI 10.1007/s11164-013-1293-y (2013)**
15. K. Adardour, R. Touir, M. El Bakri, Y. Ramli, M. Ebn Touhami, H. El Kafsaoui, C. Kalonji Mubengayi, E. M. Essassi. **Res. Chem. Intermed., DOI 10.1007/s11164-012-0934-x (2012)**
16. K. Adardour, R. Touir, Y. Ramli, R.A. Belakhmima, M. Ebn Touhami, C. Kalonji Mubengayi, H. El Kafsaoui, E.M. Essassi**. Res. Chem. Intermed. DOI:10.1007/s11164-012-0719-22144 (2012)**
17. H. Zarrok, A. Zarrouk, R. Salghi, Y. Ramli, B. Hammouti, S.S. Al-Deyab, E.M. Essassi, H. Oudda. **Int. J. Electrochem. Sci. 7, 8958–8973 (2012)**
18. M. Elbakri, R. Touir, M. Ebn Touhami, A. Zarrouk, Y. Aouine, M. Sfaira, M. Bouachrine, A. Alami, A. El Hallaoui. **Res. Chem. Intermed., DOI 10.1007/s11164-012-0768-6 (2012)**
19. F. Bentiss, M. Traisnel, M. Lagreneé. **J. Appl. Electrochem, 31, 41 (2001)**
20. M.S. Al-Otaibia, A.M. Al-Mayoufa, M. Khana, A.A. Mousaa, S.A. Al-Mazroab, H.Z. Alkhathlana. **Arabian Journal of Chemistry, 7, 340–346 (2014)**
21. I.N. Putilova, S.A. Balezin, V.P. Barannik. **Metallic Corrosion Inhibitors, Pergamon Press, London, 125 (1960).**
22. I. Sekine, Y. Nakahata, H. Tanabe. **Corros. Sci. 28, 987 (1988).**
23. B.G. Clubley. **Chemical Inhibitors for Corrosion Control, Royal Society of Chemistry, Cambridge, 110, (1990)**
24. I.B. Singh, G. Venkatachari, K. Balakrishnan. **J. Appl. Electrochem. 24, 179 (1994)**
25. L.M. Rodriguez-Valdez, A. Martinez-Villafane, D. Glossman-Mitnik, CHIH-DFT**. J. Mol. Struct. (Theochem) 716, 61–65 (2005).**
26. R. Touir, M. Cenoui, M. El Bakri, M. Ebn Touhami. **Corros. Sci., 50, 1530–1537 (2008)**
27. R. Touir, M. El Bakri, N. Dkhireche, M. Ebn Touhami, A. Rochdi. **J. Mater. Environ. Sci. 1, 317-328 (2010)**
28. R. Touir, N. Dkhireche, M. Ebn Touhami, M. Lakhrissi, B. lakhrissi, M. Sfaira. Desalination, 249, 922-928 (2009)
29. ASTM G-81, **Annual Book of ASTM Standards, (1995)**
30. M.S. Abdel Aal, S. Radwan, A. El Saied. **Br. Corros. J,18, 2 (1983)**
31. A. Boukamp. **Users Manual Equivalent Circuit, ver. 4.51, (1993)**
32. R.S. Chaudhary, S. Sharma. **Indian J. Chem. Technol, 6, 202 (1999).**
33. F. Bentiss, M. Traisnel, M. Lagreneé**. Appl. Surf. Sci., 161, 196 (2000).**
34. M.A. Quraishi, D. Jamal. **Mater. Chem. Phys, 78, 608 (2003).**
35. M.A. Quraishi, H.K. Sharma**. Mater. Chem. Phys, 78, 18 (2002).**
36. B.G. Ateya, M.B.A. El-Khair, I.A. Abdel-Hamed. **Corros. Sci, 16, 163 (1976).**
37. W. Li, Q. He, S. Zhang, C. Pei, B. Hou. **J. Appl. Electrochem, 38, 289 (2008).**
38. M.A. Quraishi, S. Ahmad, G. Venkatachari. **Bull. Electrochem, 12, 109 (1996)**
39. S. Ghareba, S. Omanovic. **Corros Sci, 52, 2104 (2010).**
40. B. Mernari, L. Elkadi, S. Kertit. **Bull. Electrochem, 17, 115 (2001)**
41. C.H. Hsu, F. Mansfeld. **Corrosion, 57, 747–748 (2001)**
42. J. Cruz, T. Pandiyan, E.G. Ochoa. **J. Electroanal. Chem, 8, 583 (2005)**
43. D.A. Lopez, S.N. Simison, S.R. Sanchez. **Corros. Sci, 47, 735 (2005)**
44. J.W. Schultze, K. Wippermann**. Electrochim. Acta, 32, 823 (1987)**
45. S. Martinez, M. Metikos-Hukovic. **J. Appl. Electrochem, 33, 137 (2003).**

46. R. Raicheff, K. Valcheva, E. Lazarova. **Proceeding of the Seventh European Symposium on Corrosion Inhibitors, 48, (1990)**
47. F. Bentiss, M. Lebrini, M. Lagrenée, M. Traisnel, A. Elfarouk, H. Vezin. **Electrochim. Acta, 52, 6865 (2007).**
48. K.F. Khaled**. Electrochim. Acta, 53, 3484 (2008)**
49. M. Elayyachy, A. El Idrissi, B. Hammouti. Corros. Sci, 48, 2470 (2006)
50. G. Avci. Mater. **Chem. Phys, 112, 234 (2008)**
51. E. Bayol, A. A. Gurten, M. Dursun, K. Kayakırılmaz. **Acta Phys. Chim. Sin, 24, 2236 (2008)**
52. O.K. Abiola, N.C. Oforka. **Mater. Chem. Phys, 83, 315 (2004)**
53. M. Ozcan, R. Solmaz, G. Kardas, I. Dehri. **Colloid Surf. A, 57, 325 (2008)**
54. F. Hongbo. **Chemical Industry Press, Beijing, 166 (2002).**
55. S.A. Ali, H.A. Al-Muallem, M.T. Saeed, S.U. Rahman. **Corros. Sci. 50, 664 (2008)**
56. E.S. Ivanov. **Inhibitors for Metal Corrosion in Acid Media (Metallurgy, Moscow) (1986)**
57. N.P. Zhuk. **Course on Corrosion and Metal Protection (Metallurgy, Moscow) (1976)**
58. A. Popova. **Corros. Sci, 49, 2144– 2158 (2007)**
59. I. Putilova, S. Balezine, V. Barannik**. in Metalic Corrosion Inhibitors, ed. by E. Bishop (London,England, (1960).**
60. F. Bentiss, M. Traisnel, L. Genegembre, M. Lagrenée. **Appl. Surf. Sci. 152, 237 (1999).**
61. A. Popova, E. Sokolova, S. Raicheva, M. Christov. **Corros. Sci., 45, 33 (2003)**
62. L. Herrag, B. Hammouti, S. Elkadiri, A. Aouniti, C. Jama, H. Vezin, F. Bentiss. **Corros. Sci., 52 3042–3051 (2010)**
63. J. Marsh. **Advanced Organic Chemistry, 3rd edn. Wiley Eastern, New Delhi (1988)**
64. S. Martinez, I. Stern**. Appl. Surf. Sci, 199, 83 (2002)**
65. M. Dahmani, A. Et-Touhami, S.S. Al-Deyab, B. Hammouti, A. Bouyanzer. **Int. J. Electrochem. Sci, 5 1060 (2010)**